HYDROLOGICAL PROCESSES
Hydrol. Process. **18**, 3609–3622 (2004)
Published online in Wiley InterScience (www.interscience.wiley.com). DOI: 10.1002/hyp.5804

Ground-based frequency-modulated continuous wave radar measurements in wet and dry snowpacks, Colorado, USA: an analysis and summary of the 2002–03 NASA CLPX data

Hans-Peter Marshall,[1,2]* Gary Koh[3] and Richard R. Forster[4]

[1] *Institute of Arctic and Alpine Research and Department of Civil, Environmental, and Architectural Engineering, University of Colorado at Boulder, Boulder, CO 80309-0450, USA*
[2] *Swiss Federal Institute for Snow and Avalanche Research (SLF), CH-7260 Davos Dorf, Switzerland*
[3] *US Army Cold Regions Research and Engineering Laboratory, Hanover, NH 03755-1290, USA*
[4] *Department of Geography, University of Utah, Salt Lake City, UT 84112-9155, USA*

Abstract:

Ground-based frequency-modulated continuous wave (FMCW) radar measurements made throughout the 2002–03 NASA Cold Lands Processes (CLPX) mission in Colorado, USA, were designed to study the major electromagnetic transitions within the alpine snowpack over a wide range of conditions, and their effect on measurements made with different active radar measurement parameters. Measurements during 2002 determined that measurements at C-, X-, and Ku-band frequencies were necessary to retrieve the most snowpack information in a wide range of conditions. Measurements at four different incidence angles indicated that the snowpack layering was still visible at 15° but that the rough surface scattering of the snow–ground interface dominated the signal above 30° incidence. Measurements during 2003 were focused on characterizing the microwave response at C-, X-, and Ku-band frequencies at four different sites with different snowpack conditions, indicating that the optimal measurement parameters vary with snowpack conditions. Measurements at different bandwidths illustrate the effect of bandwidth on vertical resolution. This ground-truth data will help interpretation of air- and space-borne active and passive microwave radar measurements that were made coincident with this study. In addition, this work may help guide future researchers when choosing FMCW radar measurement parameters, depending on the type of snowpack information their study requires. Copyright © 2004 John Wiley & Sons, Ltd.

KEY WORDS snow; microwave radar; snow water equivalent (SWE); remote sensing; CLPX

INTRODUCTION

The NASA Cold Land Processes (CLPX) mission (2002–03) was designed to enhance our knowledge of the terrestrial cryosphere, by improving our ability to measure snowpack and soil properties remotely (Cline, 2000). One of the major objectives of this large-scale study, which spanned several disciplines and involved researchers from many universities and institutions, is to evaluate and improve radar retrieval algorithms for snow depth, density, wetness, and total snow water equivalent (SWE). In order to invert snow-cover properties accurately from active and passive microwave remote-sensing measurements, it is important to separate the effect of mean snowpack properties from the effect of snowpack layering. Strong dielectric discontinuities within the snow can obstruct the microwave energy emitted from the ground, thus reducing the brightness temperature of a snowpack. In addition, active microwave signals are reflected and scattered from these layer boundaries and, therefore, radar backscatter signatures are largely effected by snowpack layering.

* Correspondence to: Hans-Peter Marshall, INSTAAR, University of Colorado at Boulder, 1560 30th St, Campus Box 450, Boulder, CO 80309, USA. E-mail: marshalh@colorado.edu

Received 15 June 2004
Accepted 10 September 2004

The NASA CLPX 2002–03 mission was designed to address scaling issues that arise when comparing narrowband spaceborne measurements (which are averaged over many metres in the horizontal and represent an average over the thickness of the snowpack) with point snowpit measurements of SWE. Detailed measurements were made in a series of regions with different length scales, in Colorado, USA, during the 2002 and 2003 winters. Three intensive study areas (ISAs) were chosen in the Colorado Rockies to represent the different snowpack conditions found in continental climates. Measurements were made in February and March of each year, for a total of four intensive observation periods (IOPs), in order to cover both wet and dry snowpack conditions. At the local-scale observation site (LSOS), detailed measurements with many different instruments were made by investigators spanning many disciplines and institutions. A large team of surveyors made snowpit measurements throughout all three ISAs during each IOP while air- and space-borne measurements were made in each area.

In order to aid interpretation of both active and passive remote-sensing measurements made during the CLPX mission, we performed ground-based frequency-modulated continuous wave (FMCW) measurements. Measurements were made in four different snowpacks, with depths ranging from 40 to 336 cm, which were both wet and dry, to characterize the range of snowpacks present across the study area of the CLPX mission. We also made detailed measurements of snowpack properties in an adjacent snowpit at each site. The FMCW technique offers the ability to transmit over both a broad bandwidth (which allows high vertical resolution) and at more narrow bandwidths (which simulate airborne measurements). Measurements made at high vertical resolution made it possible to locate the cause of the major reflections that come from within the snowpack, and combined with narrowband measurements these can help to estimate the effect of snowpack layering on the total backscatter measured by aircraft or satellite.

The electromagnetic response of the snowpack is sensitive to the centre frequency transmitted; therefore, we made measurements at C- (2–6 GHz), X- (8–12 GHz), and Ku-band (14–18 GHz) frequencies. Remote-sensing platforms often make off-nadir measurements; therefore, we also made ground-based FMCW measurements at four different incidence angles ($\theta = 0$, 15, 30, 45°) in each of the frequency ranges. *In situ* electrical properties were measured in nearby snowpits at several sites, and metal reflectors were used to pinpoint the snowpack depths of major radar reflections.

BACKGROUND

As a more thorough summary of previous FMCW radar work in snow has been given elsewhere (e.g. Marshall *et al*., 2004b), here we briefly indicate the major studies. Ellerbruch and Boyne (1980) were the first to publish results of FMCW measurements in alpine snow. Using a measurement of mean density $\overline{\rho_s}$, they were able to estimate snow depth d to $\pm 5\%$ at many sites, noted strong reflections from depth hoar layers, and measured changes in reflectivity during melting. Gubler and Hiller (1984) built an FMCW system to measure speeds and heights of avalanches, discussed the effect of layer thickness on reflectivity, and measured mean density $\overline{\rho_s}$ to within $\pm 5\%$ using a measurement of snow depth d.

FMCW measurements have also been combined with the snowpack model SNTHERM (Koh and Jordan, 1995) to demonstrate that near-surface melting when temperatures were near but not above freezing could be detected in the FMCW signal. Koh *et al*. (1996) showed that a multi-band approach is necessary for using FMCW radar to monitor the entire snowpack in a wide range of conditions. Holmgren *et al*. (1998) used an X-band FMCW radar to measure snow depth over long traverses.

Microwave FMCW radar responds to changes in dielectric properties within the snowpack, as major reflections have been shown to be highly correlated with changes in dielectric properties measured *in situ* in a nearby snowpit (Marshall *et al*., 2004b). Using metal reflectors inserted at layer boundaries, this study also showed that the major reflections often coincide with boundaries observed visually in a nearby snowpit, and that using the mean density to approximate the velocity of propagation leads to an error in the depth scale of less than 2%. Using a typical dry snow dielectric constant, Marshall *et al*. (2004b) were able to estimate SWE to within 10%.

THEORY

Since the airborne active radar measurements made as part of the CLPX mission were in the microwave region, it was important to have the ground-based radar measurements in the same frequency range. Commercial pulsed radars are only available up to a frequency of 2 GHz currently, as digital-to-analogue converters above this frequency are prohibitively expensive. The FMCW technique has the advantage of enabling a measurement to be made at much higher frequencies, while using a sample frequency several orders of magnitude lower. FMCW radars can also operate over a much larger bandwidth, resulting in very high vertical resolution.

As the theory of FMCW radar has also been discussed previously (e.g. Stove, 1992), just a brief description of the technique is given below. The transmitted (chirp) signal has a frequency f that varies linearly with time over a bandwidth B for the duration of the pulse T_{pl}. A sample of this transmitted signal is mixed (multiplied) by the received signal before sampling, resulting in a signal that contains the difference in frequency Δf between the two signals. This frequency difference, due to the linearity of the transmitted signal, is proportional to the distance d to a given reflector

$$d = \frac{1}{2} v_{\mathrm{s}} T_{2w} = \frac{1}{2} v_{\mathrm{s}} \left(\Delta f \frac{T_{\mathrm{pl}}}{B} \right) \tag{1}$$

where $v_{\mathrm{s}} = c/\sqrt{\overline{\varepsilon_{\mathrm{s}}}}$ is the velocity of propagation in snow, c is the speed of light in a vacuum, and the average dielectric constant of the snowpack is $\overline{\varepsilon_{\mathrm{s}}}$. For a typical required maximum range $d_{\max}$ of 1–10 m, this frequency difference Δf is in the kilohertz range. This means that the digital-to-analogue converter can operate at a frequency several orders of magnitude below the transmitted frequency range.

METHODS

The NASA CLPX mission spanned four IOPs during 2002–03, with measurements performed throughout a large area (4·5° × 3·5°), covering the wide range of snowpack conditions typical of a continental climate (Figure 1). During the first two campaigns (IOPs 1 and 2), the ground-based FMCW radar measurements were focused at the LSOS in the Fraser Experimental Forest (−105·88 306 Lat, 39·90 172 Lon). Detailed measurements were made at C- (2–6 GHz), X- (8–12 GHz), and Ku-band (14–18 GHz) frequencies, and at incidence angles $\theta = 0$, 15, 30, and 45°. This area has a mid-sized (~1 m) snowpack, and measurements were also made with numerous instruments by many different groups at this site as part of CLPX (active/passive radar, automatic weather stations, snowpits, spectrometer, etc.). During IOP 1 in February 2002 the snowpack was dry, and during IOP 2 in March 2002 it was wet. FMCW measurements were made from a motorized tripod, located at a height of approximately 1 m above the snow surface.

During the second two campaigns (IOPs 3 and 4) in February and March of 2003, measurements were made at four different sites to cover the wide range of snowpack conditions: LSOS, Berthud Pass, Michigan Ridge (North Park), and Buffalo Pass (Steamboat Springs). The locations of each site are given in Table I. Although the FMCW system used still required AC power, a generator was used at all of the sites besides LSOS. At each site, measurements were made at C-, X-, and Ku-band frequencies. These data from IOPs 1–4 have all been documented, processed, and delivered to the National Snow and Ice Data Center (NSIDC) (Marshall *et al*., 2004a) and are listed in Table II. Measurements were also made at four incidence angles and three different bandwidths; however, these measurements have not yet been processed.

A snowpit was excavated directly adjacent to the FMCW measurements, and measurements of the layering, grain size and type, hand hardness, density, and temperature were made. At several of the sites, *in situ* electrical

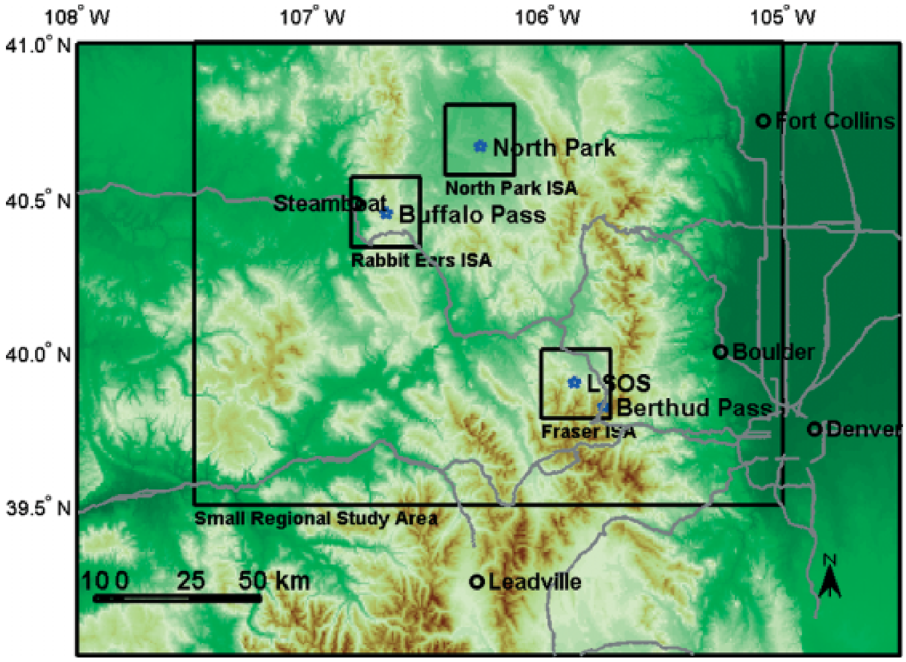

Figure 1. Colorado, USA. The large box shows the CLPX small regional study area, and the small boxes indicate the boundaries of the three ISAs. Circles show locations of major cities and stars indicate the four sites visited during IOPs 3 and 4

Table I. CLPX site locations

Name	MSA	Lat	Lon
LSOS	Fraser	−105·88306	39·90172
Michigan Ridge	North Park	−106·18060	40·64487
Berthud Pass	Frasier	−105·76808	39·82797
Buffalo Pass	Rabbit Ears	−106·67881	40·53816

Table II. List of data sets collected during NASA CLPX 2002/2003

Site	Date	Measurements/notes
LSOS	19 Feb 2002, 21 Feb 2002, 24 Mar 2002, 26 Mar 2002	$\theta = 0°$, f = C, X, Ku
LSOS	21 Feb 2002	$\theta = 0$, 15, 30, 45°, f = C, X, Ku
LSOS	19 Feb 2003	C, X, Ku
LSOS	20 Feb 2003	C, X, Ku @ 08:00, 12:30, 15:00
Michigan Ridge	21 Feb 2003	C, X (Ku-horns broke)
Berthud Pass	22 Feb 2003	C, X, Ku
Buffalo Pass	23 Feb 2003	C, X, Ku
LSOS	25 Mar 2003	C (A/D converter broke)
LSOS	28 Mar 2003	C, X, Ku
Buffalo Pass	29 Mar 2003	C, X, Ku

properties were measured with a Finnish Snowfork (Tiuri *et al.*, 1984). Experiments were also performed with a metal reflector placed at specific locations in the wall of the snowpit, to pinpoint the snowpack depths of reflections in the radar signal.

Processing

Each data set consists of a set of measurements of voltage as a function of time $v(t)$, made during a transmitted pulse. This signal is converted to the frequency domain via a zero-padded, windowed fast-Fourier transform:

$$P(\omega) = \int W\ v(t)\ \mathrm{e}^{-\mathrm{i}\omega t}\ \mathrm{d}t \tag{2}$$

where W is the window function, ω is the frequency, and $P(\omega)$ is the power spectral density at each frequency and is directly related to the strength of the reflection at the associated depth.

This power spectral density function $P(\omega)$ contains signals associated with the instrumentation and signals associated with the snowpack. Using a sky calibration measurement (horn antennas pointed at the sky) and a filtering algorithm, we next remove most of the instrumentation-related signals. The resulting signal is converted to power spectral density as a function of depth $P(d)$ using Equation (1). For each of the nadir measurements ($\theta = 0$), the signal was next normalized to the power spectral density associated with the reflection from the surface of the snow

$$P_{\mathrm{dB}}(d) = 10\ \log\left(\frac{P(d)}{P(d = \mathrm{surface})}\right) \tag{3}$$

where $P_{\mathrm{dB}}(d)$ is the relative power spectral density, and $P(d = \mathrm{surface})$ is the power reflected from the snow surface. For the off-nadir measurements ($\theta = 15$, 30, 45°) the signal was normalized to the signal from a standard calibration target

$$P_{\mathrm{dB}}(d) = 10\ \log\left(\frac{P(d)}{P_{\mathrm{cal}}}\right) \tag{4}$$

RESULTS

Experiments were performed successfully with a very wide range of measurement parameters during IOPs 1 and 2 at the LSOS site (Figure 1, Table I, Table II). Guided by the results from IOPs 1 and 2, measurements at C-, X-, and Ku-band frequencies were made in four different snowpacks during IOPs 3 and 4. The date and location of each successful measurement are given in Table II and the location of each site is shown in Figure 1 and Table I. This resulted in an enormous amount of data, and here we indicate the breadth of information this dataset contains by showing a subset to demonstrate the effect of various measurement parameters and snowpack conditions.

Frequency effect

Measurements made at C-, X-, and Ku-band frequencies demonstrate the trade-off between received signal strength and sensitivity to the contrast of layer electrical properties. In order to isolate the effect of frequency, the following measurements were all made with a bandwidth B of 4 GHz and, therefore, have the same vertical resolution Δz. In a dry snowpack, we were not always able to see the ground reflection at Ku-band frequencies; however, this highest frequency band showed the most sensitivity to subtle transitions, as it always showed reflections from more layers than the measurements at lower frequencies did. An example is shown in Figure 2, where all measurements were made in the same location. The data shown are an average of measurements taken over a 4 m horizontal scan.

FMCW measurements from all three frequency bands have been normalized to the reflection from the snow surface. All three measurements have an identical surface reflection in this plot, and the curves all overlap

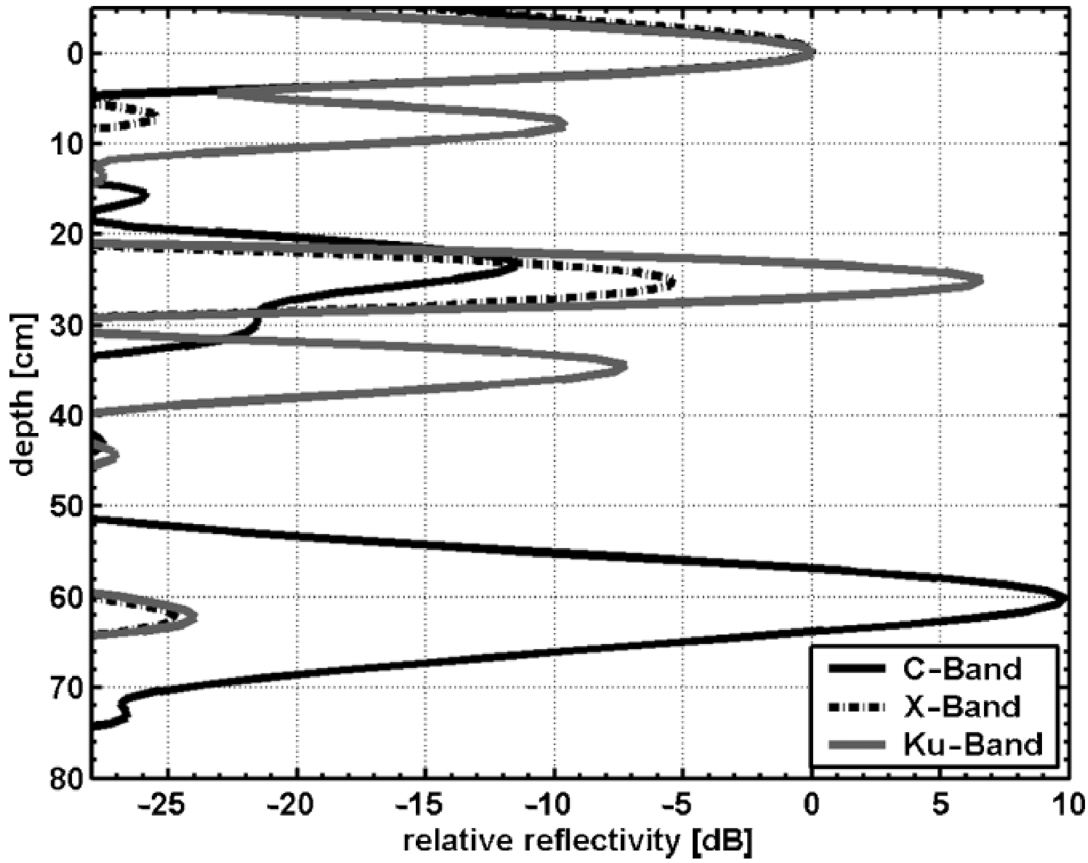

Figure 2. Effect of frequency in dry snow. All measurements made with a bandwidth of 4 GHz; therefore, they have the same vertical resolution. The surface reflection at 0 cm overlaps for all three measurements. C-band frequencies show the largest ground reflection, whereas Ku-band frequencies are the most sensitive to subtle layering

here. The solid black line shows measurements made in the lowest frequency range, 2–6 GHz. Note that there is a surface reflection, one mid-pack reflection, and a very strong ground reflection at ~60 cm, which is larger than that from the surface. In all of the measurements made during the NASA CLPX mission, C-band frequencies in dry snow penetrate well and always show a strong ground reflection that is often larger than the signal from the surface. Measurements at X-band (8–12 GHz), shown with a dashed black line, also show surface, ground, and mid-pack reflections at the same locations. These measurements have a much lower amplitude ground reflection, but also show one additional reflection at ~10 cm. At Ku-band (14–18 GHz), shown in grey, note that the surface, ground, and mid-pack reflections are consistent; in addition, there are two other reflections from within the snowpack. Note also that the ground reflection is just as strong as that from the X-band measurement. This indicates that Ku-band measurements are the most sensitive to subtle transitions and, therefore, give the maximum layering information, while C-band measurements give a strong reflection from the snow–ground interface.

These same measurements were repeated 1 month later, during IOP 2, at the same location, where the snowpack had experienced significant warming and was now mostly wet. The results of the average measurement in each frequency range are shown in Figure 3. Here, the C-band measurements still penetrate the snowpack, as indicated by the ground reflection at ~60 cm, and a mid-pack layer is also still visible. X-band measurements do not resolve the snow–ground interface, but still have a strong reflection from the

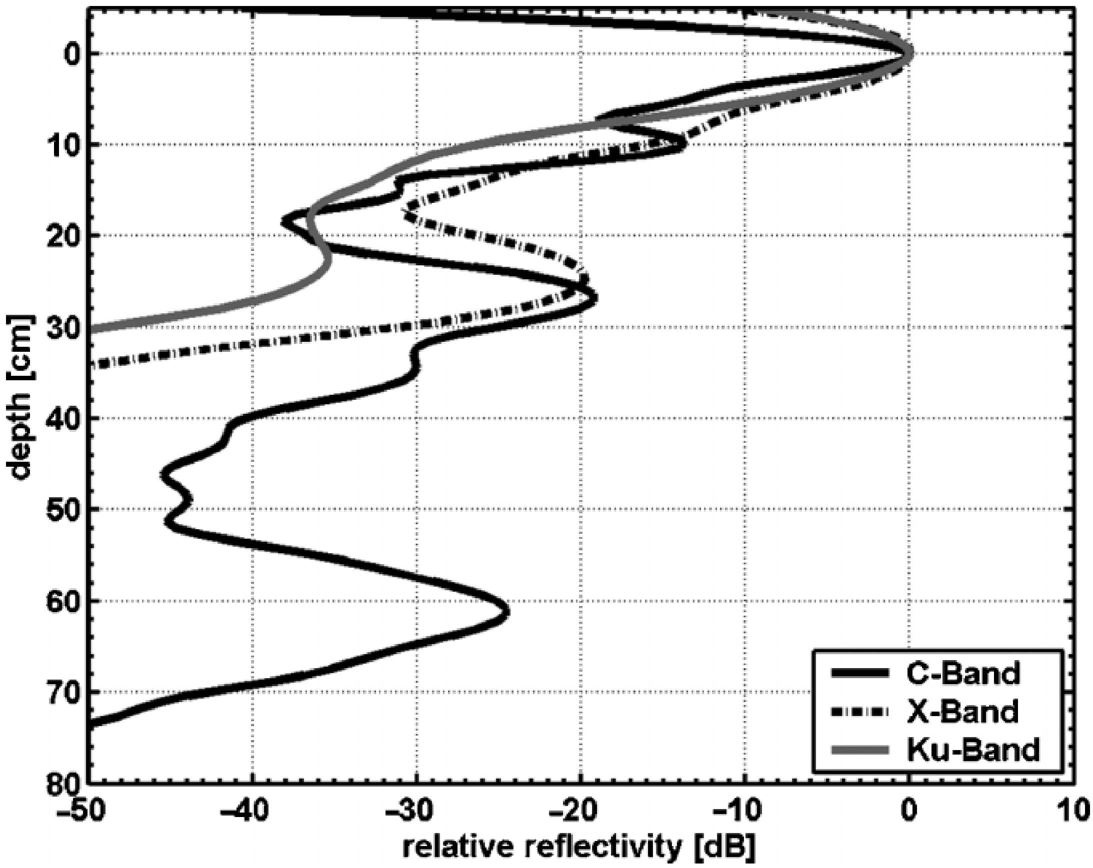

Figure 3. Effect of frequency in wet snow. All measurements made with a bandwidth of 4 GHz; therefore, they have the same vertical resolution. The surface reflections overlap, and only C-band frequencies have a ground reflection at ~60 cm. Ku-band frequencies are rapidly attenuated, and the signal is dominated by the reflection from the surface

mid-pack transition at ~25 cm depth. The measurements at Ku-band show rapid attenuation, as the majority of the signal power is coming from the upper 10 cm of the snowpack. These measurements indicate that C-band frequencies are necessary for penetrating a wet snowpack, whereas measurements at Ku-band frequencies in wet snow are dominated by the surface reflection. These two sets of measurements indicate that both C- and Ku-band frequencies are ideal for FMCW radar in a wide range of snowpack conditions.

Bandwidth effect

Increasing the transmitted frequency increases sensitivity to transitions within the snowpack. The resolution of the signal, or the minimum separation at which two layer transitions can be distinguished, however, is a function of the bandwidth of the transmitted chirp. Measurements made over a wider bandwidth result in sharper peaks. Figure 4 shows measurements made at C-band frequencies, with bandwidths of 1 and 4 GHz. The theoretical resolution of the FMCW signal is

$$\Delta z = \frac{v_s}{2B} = \frac{c}{2B\sqrt{\overline{\varepsilon_s}}} \tag{5}$$

where v_s is the mean velocity of propagation in the snowpack, B is the bandwidth, and $\overline{\varepsilon_s}$ is the mean dielectric constant of the snow. Using our system bandwidths of 1 GHz and 4 GHz, and the mean dielectric constant

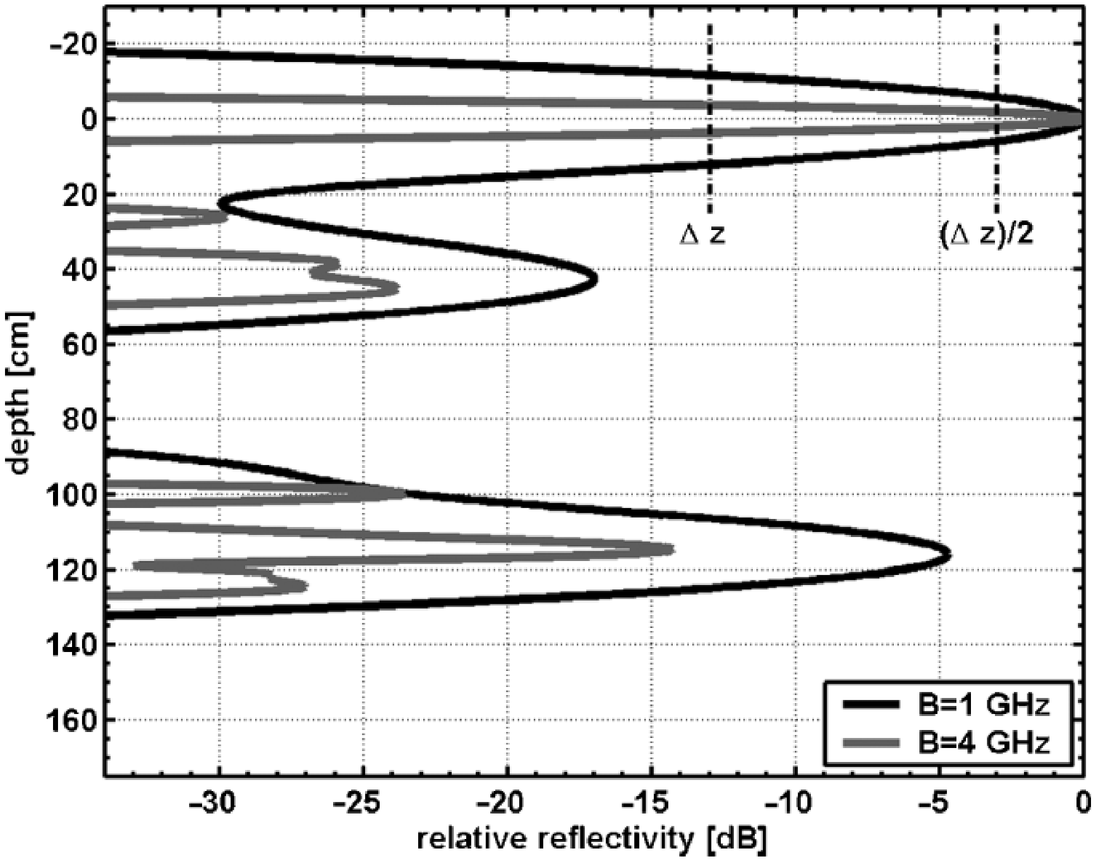

Figure 4. Effect of bandwidth on resolution. Both measurements made at C-band frequencies. The location at which the surface reflection has a half-width equal to the theoretical bandwidth $\Delta z = v_s/2B$ is shown, as is the location at half this value ($\Delta z/2$)

of this snowpack, Equation (5) gives resolutions Δz of 12·5 cm and 3·1 cm respectively. In the measurement shown in Figure 4, the location where the two signals' half-widths are equal to this resolution Δz is shown with a dashed line on the surface reflection at -13 dB. This indicates that, with our system, this theoretical resolution Δz corresponds to the minimum separation at which two signals, which differ by a factor of 20, can be resolved. If the signals only differ by a factor of 2, then this resolution is about half as small, as shown by the other dashed line on the surface reflection at -3 dB. This means that two reflectors that are closer than Δz and that differ in magnitude by more than a factor of 20 will be indistinguishable using a system with a bandwidth less than B. This effect can make it difficult to distinguish ice lenses from ground reflections in narrowband radar measurements.

Effect of incidence angle θ

We also made measurements at a variety of incidence angles. This was done both for simulating airborne measurements and for qualitatively determining the relative contributions of surface and volume scattering. C-band measurements at an incidence angle $\theta = 0$, 15, 30, and 45° are shown in Figure 5. These measurements were normalized based on the reflectivity of a standard calibration target, and are shown with a vertical scale that represents the approximate depth in the snowpack. This depth d_s takes into account the path length for the different measurements, but not refraction effects, and is calculated as

$$d_s = d \cos(\theta) \tag{6}$$

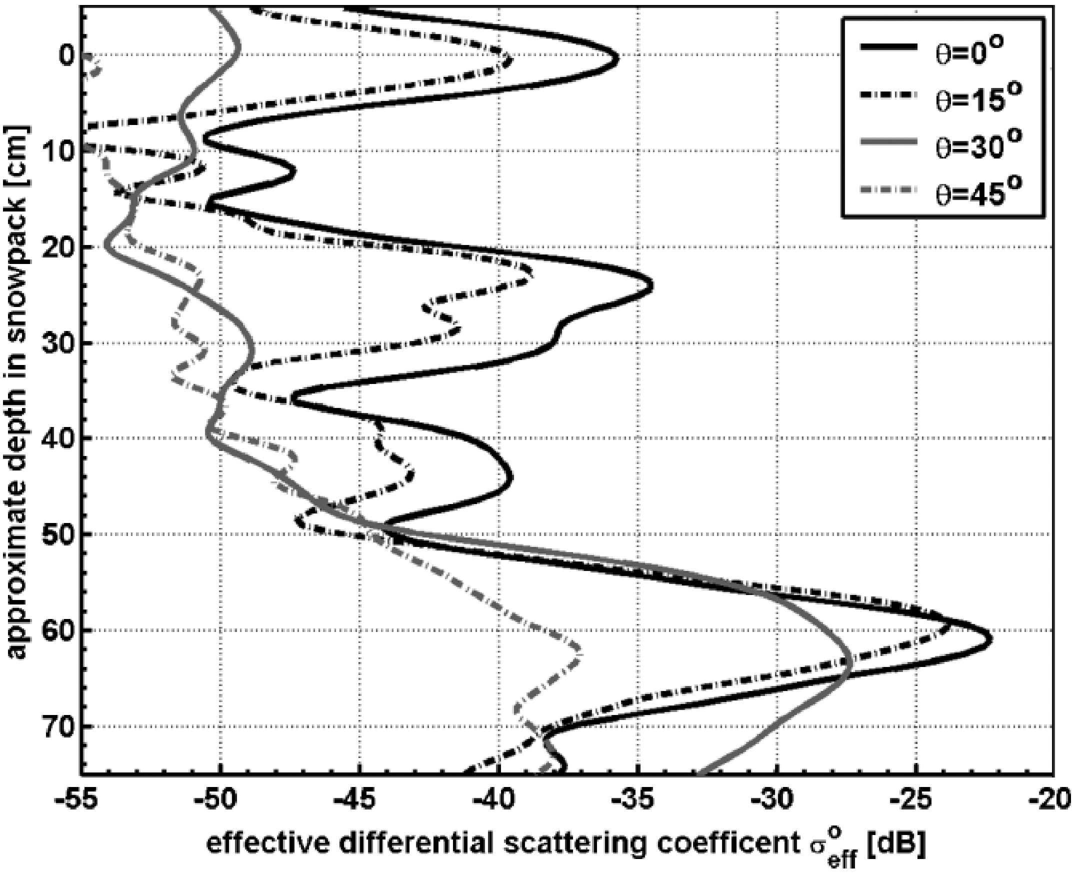

Figure 5. Effect of incidence angle θ. The vertical axis is the depth within the snowpack, corrected for path length but not refraction. Snowpack layering is still visible at $\theta = 15°$, but measurements at $\theta = 30$ and $45°$ are dominated by the ground reflection

where d is the actual distance to the reflector, θ is the incident angle, and d_s is the approximate snowpack depth.

The measurement made at $\theta = 0°$ is shown with the solid black line. Clearly visible are the surface reflection, two mid-pack reflections, and a ground reflection at ~60 cm. In the data from $\theta = 15°$, shown with a dashed black line, the surface and two mid-pack layers are still visible, as is the ground reflection. Snowpack stratigraphy is still measurable at this incidence angle, and also note that, owing to the actual increased path length, this measurement shows higher resolution and appears to be separating two separate reflections from each of the mid-pack layers.

At an incidence angle of $\theta = 30°$ the surface is still visible, along with a large ground reflection; however, the snowpack stratigraphy is difficult to interpret. A relatively small reflection is visible from the major mid-pack transition. At an incidence angle $\theta = 45°$ the signal is coming almost entirely from the ground. These kinds of measurement can be used to determine the relative effects of surface and volume scattering. This experiment indicates that snow stratigraphy can still be measured at an incidence angle $\theta = 15°$; however, measurements at $\theta = 30$ and $45°$ are dominated by the reflection from the snow–ground interface.

Comparison of four different snowpacks

Since the measurements during the first two campaigns (IOPs 1 and 2) focused on studying the effects of different measurement parameters, the measurements during the second two campaigns (IOPs 3 and 4) were focused on measurements in snowpacks with depths varying from 40 to 336 cm, in both wet and dry conditions. The locations of these measurements are indicated in Figure 1 by stars, and the limits of the three CLPX ISAs are shown with solid boxes. The locations are also listed in Table I. To remove the effects of aspect on the measurements, all sites were chosen in flat areas with a slope of less than 2°.

In each snowpack, measurements were made in different frequency ranges (C-, X-, and Ku-bands). For comparison, we focus here on measurements made at C-band frequencies (2–6 GHz), with a bandwidth of 4 GHz to achieve maximum resolution, and at an incidence angle $\theta = 0^{\circ}$. The measurements at Ku-band frequencies (14–18 GHz) are also presented at two sites; however, Ku-band measurements were not successful at LSOS on 25 March 2003 or at Michigan Ridge on 21 February 2003 due to equipment failures.

Figures 6–9 show measurements made at each of the four sites. Each FMCW image is shown alongside measurements that were made in an adjacent snowpit. For the snowpit measurements, the density profile is shown with a solid line between circles. The grey shaded region indicates the layering visually observed in the snowpit, with the hand hardness scale shown at the top. Grain size and type are also indicated on the left-hand side. The grain type is indicated with the following notation: + is new snow, +/ is fragmented new snow, ◦ is melt–freeze crust, ∗ is rounded grains, □ is facets, and □∗ is rounded facets. The radar images are shown with white indicating a strong reflection and black indicating no reflection.

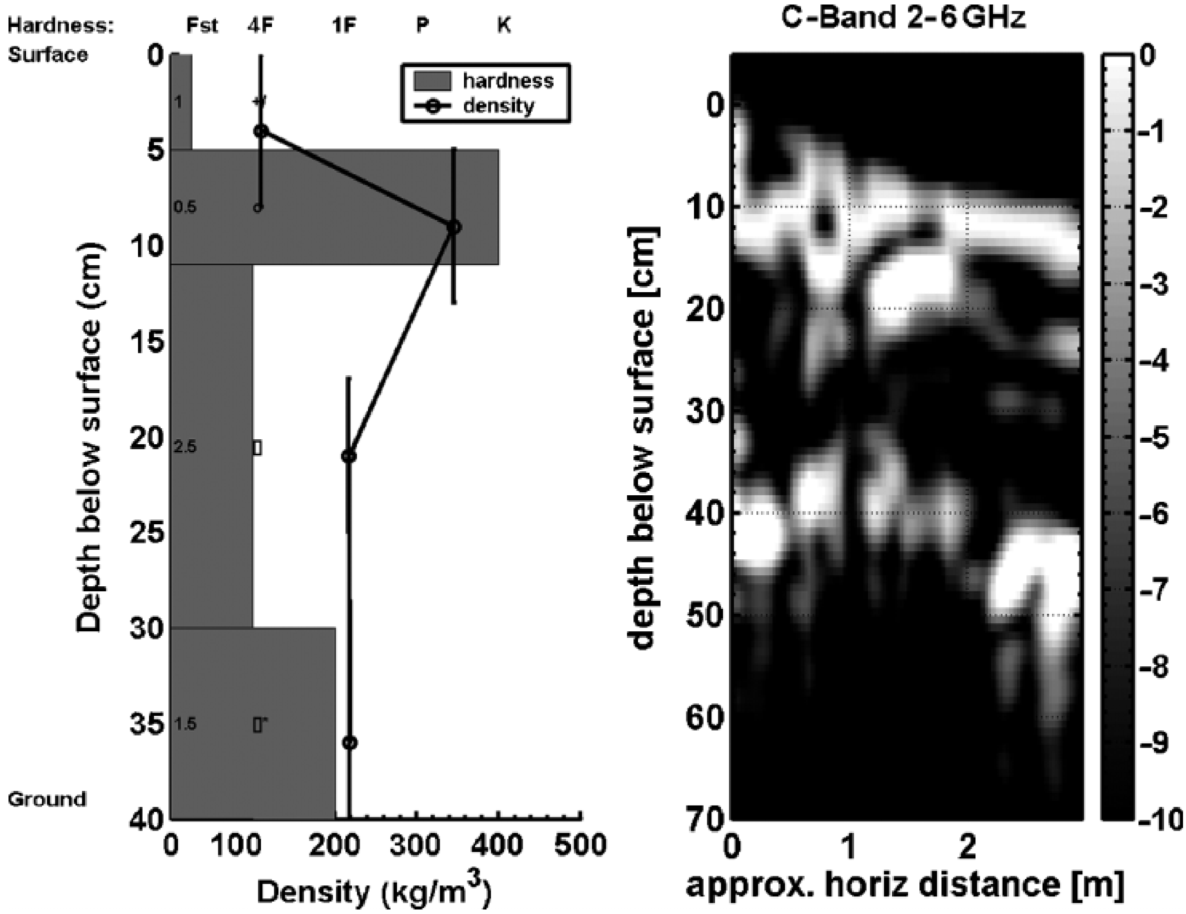

Figure 6. Shallow snowpack: Michigan Ridge, North Park (−106·18 060 Lat, 39·90 172 Lon), 21 February 2003. Radar image on the right shows C-band measurements, 2–6 GHz. White indicates a strong reflection and black indicates no reflection. Snowpit measurements are on the left, with layers shown in grey with the hardness scale at the top, and density with the solid line. Grain size and type are indicated for each layer on the left-hand side of the snowpit; see text for key to grain types

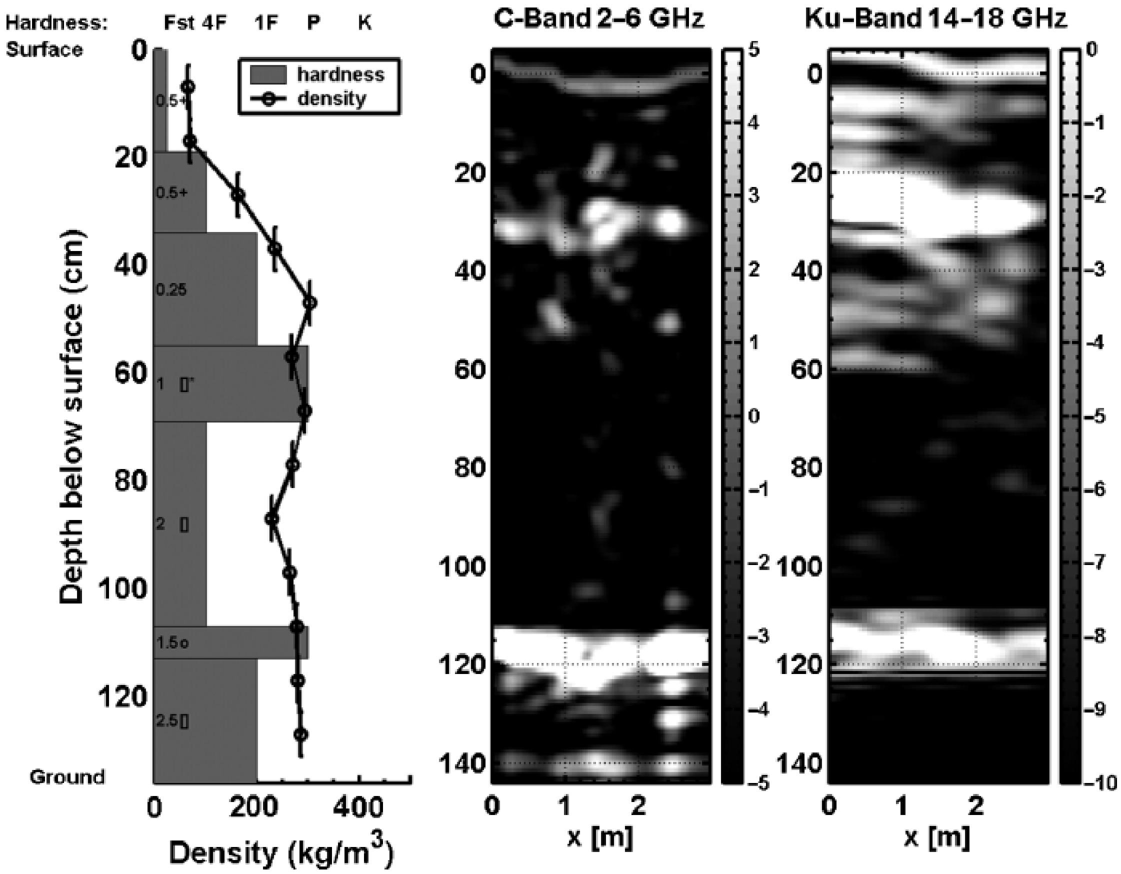

Figure 7. Mid-sized snowpack: Berthud Pass (−105·76 808 Lat, 39·82 797 Lon), 22 February 2003. Radar image in the centre shows C-band measurements, 2–6 GHz, and the image on the right shows Ku-band measurements, 14–18 GHz. White indicates a strong reflection and black indicates no reflection. Snowpit measurements are on the left, with layers shown in grey with the hardness scale at the top, and density with the solid line. Grain size and type are indicated for each layer on the left-hand side of the snowpit; see text for key to grain types

Shallow snowpack. We begin with an example of a shallow snowpack, typical of the North Park study area, shown in Figure 6 (Michigan Ridge, 21 February 2003). This is a wind-swept site, with large spatial variability in snow height. Some locations had no snow, while others had as much as 50 cm. Over the ~2 m that we scanned at this site, the snow height was relatively constant at 40 cm although the surface had a slope of ~5°, as can be seen in the radar image. The wind crust at a depth of 10 cm, identified visually in the snowpit, can be seen as a subsurface reflection on the right side of the radar image; however, it appears to be quite spatially variable. Unfortunately, the Ku-band horns broke due to high winds, so measurements in this frequency range were not successful.

Mid-sized snowpack. Next we show an example of a medium-sized snowpack, from Berthud Pass, in Figure 7 (22 February 2003). This radar image shows a surface and ground reflection in agreement with that measured in the snowpit, as well as two major internal layers. The first, at a depth of approximately 35 cm, occurs at an increase in density and hardness. The second major reflection in the radar signal is located at a depth of ~115 cm, at a melt–freeze crust and a major increase in hardness. An increase in density most likely occurred here as well; however, note that there was not a density measurement centred in this layer and, therefore, the density change was missed by the coarse resolution of our manual measurements. Note that

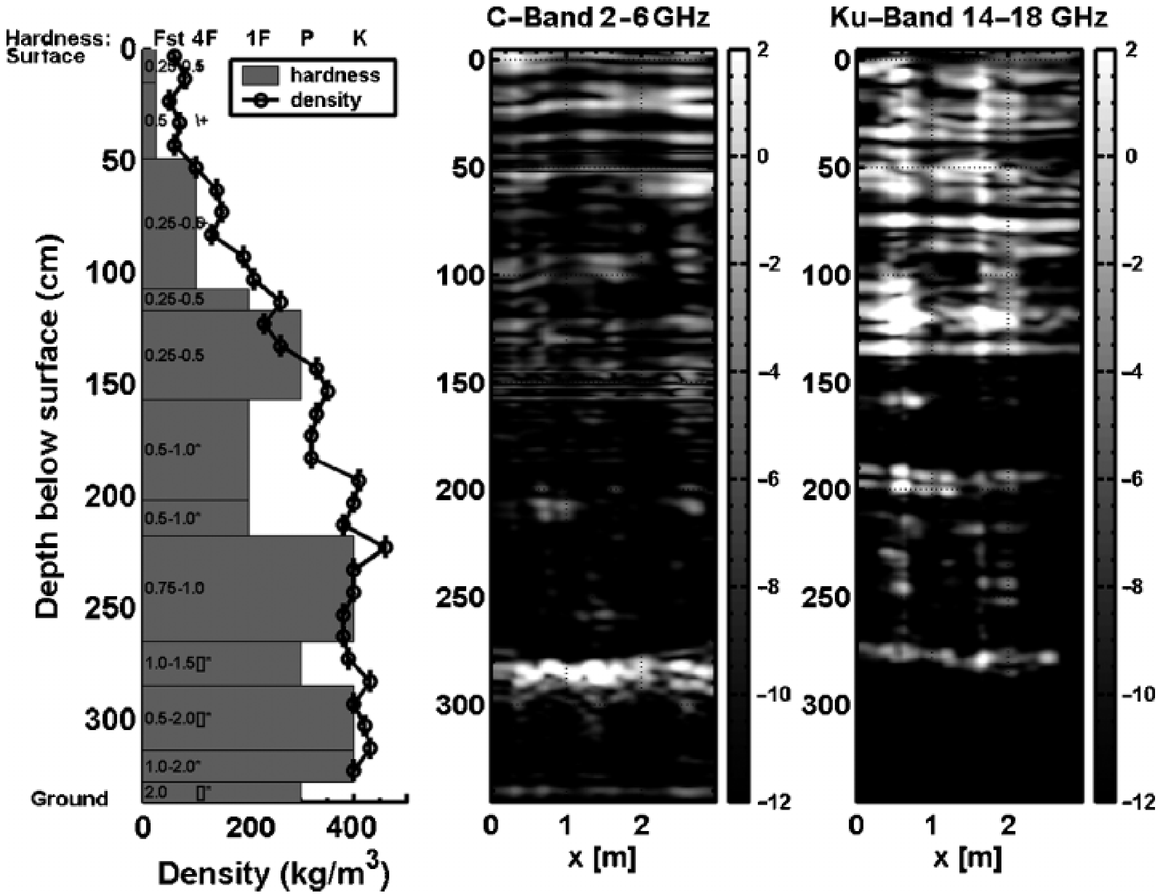

Figure 8. Deep snowpack: Buffalo Pass, Steamboat Springs (−106·67 881 Lat, 40·53 816 Lon), 23 February 2003. Radar image in the centre shows C-band measurements, 2–6 GHz, and the image on the right shows Ku-band measurements, 14–18 GHz. White indicates a strong reflection and black indicates no reflection. Snowpit measurements are on the left, with layers shown in grey with the hardness scale at the top, and density with the solid line. Grain size and type are indicated for each layer on the left-hand side of the snowpit; see text for key to grain types

more layering is visible at Ku-band frequencies, which also show a strong reflection from the melt–freeze crust but no ground reflection.

Deep snowpack. Figure 8 shows a radar scan made at Buffalo Pass, Steamboat Springs (23 February 2003). This snowpack had a depth of 336 cm, which the C-band measurement was able to penetrate, as a ground reflection (although somewhat weak) is visible at this depth. The major internal reflection occurs at a depth of approximately 280 cm, near the transition from rounded grains to faceted depth hoar. This also coincides with changes in hardness, density, and grain size. The fact that the radar shows a large return from faceted grains is encouraging, as these types of layer are very important for avalanche formation. The reflections occurring near the surface are difficult to interpret, as in this part of the snowpack the layers are nearly homogeneous, and the hardness and density are increasing nearly linearly. A linear change in dielectric properties causes a complicated effect on the radar signal (Ulaby *et al*., 1986). The Ku-band measurements show more detailed layering in the upper part of the snowpack, a very strong reflection from the transition to faceted grains, but no ground reflection.

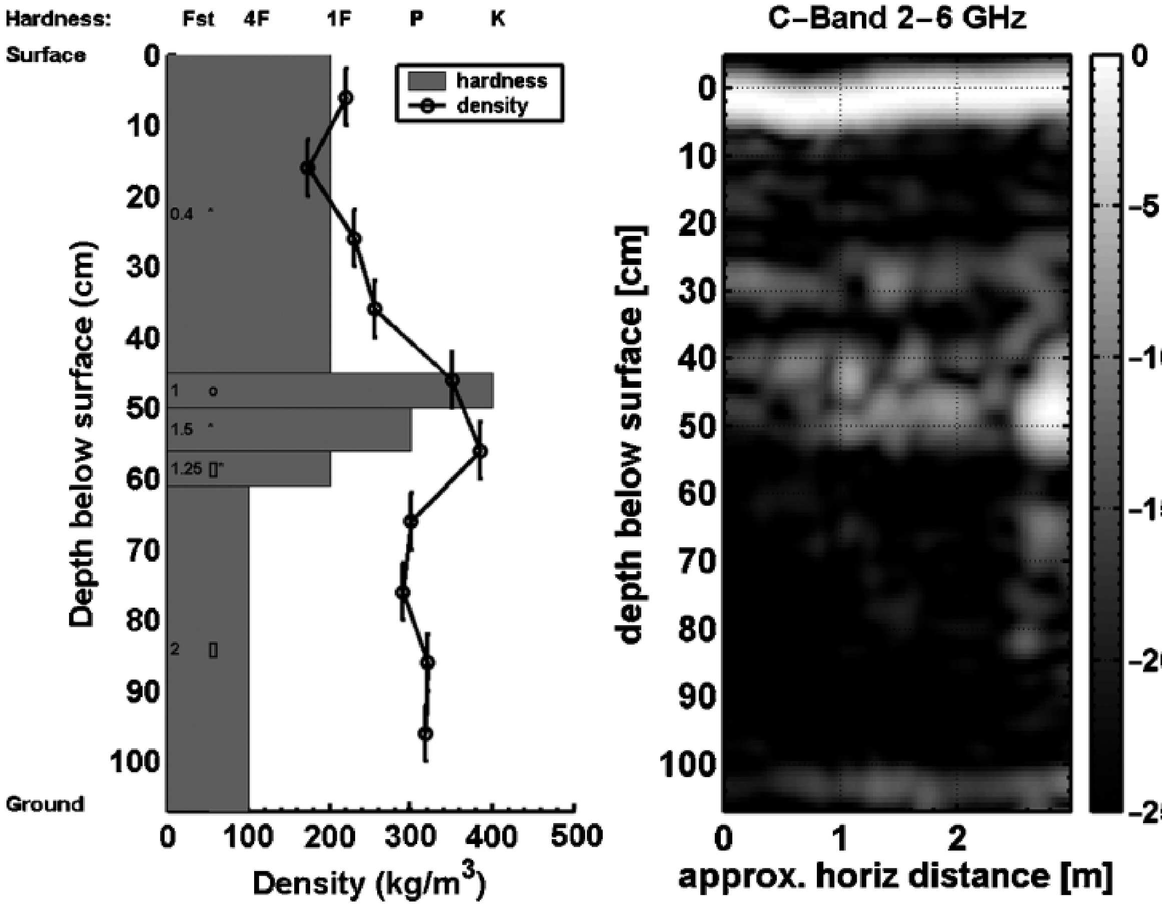

Figure 9. Mid-sized snowpack; lower half of pack has experienced warming; LSOS (−105·88 306 Lat, 39·90 172 Lon), 25 March 2003. Radar image on the right shows C-band measurements, 2–6 GHz. White indicates a strong reflection and black indicates no reflection. Snowpit measurements are on the left, with layers shown in grey with the hardness scale at the top, and density with the solid line. Grain size and type are indicated for each layer on the left-hand side of the snowpit; see text for key to grain types

Spring snowpack. In Figure 9 we show radar measurements in a spring snowpack, whose lower half has been subjected to very warm temperatures and whose upper half was formed from recent snowfall. At C-band frequencies we were still able to observe a ground reflection, although the mid-pack reflection was much larger. The mid-pack reflection occurs at a large increase in density and hardness, as well as an increase in grain size and a change in grain shape. The transition is continuous but variable; in addition, a less continuous transition, which was not observed in the snowpit layering, can be seen at a depth of ~25 cm. This may have been due to the increase in density measured at this depth. After the C-band measurements were performed, the A/D card failed and, therefore, we do not have Ku-band measurements at LSOS on 25 March 2003.

CONCLUSIONS

During the NASA CLPX mission, FMCW radar measurements were made both with a wide range of measurement parameters and in a wide range of snowpack conditions. The measurements during IOPs 1 and 2 in 2002 focused on studying the effect of measurement parameters, whereas measurements during IOPs 3 and 4 in 2003 covered the range of snowpack types observed throughout the Colorado study area.

This study indicates that, in a mid-sized dry snowpack, measurements at Ku-band frequencies (14–18 GHz) provide the most information, and still penetrate to the snow–ground interface. In deep and wet snowpacks, however, C-band frequencies perform much better. For a wide range of snowpack conditions, the optimal FMCW radar system would have the ability to operate in both of these frequency ranges. Increasing the bandwidth of the transmitted signal increases the signal complexity; however, this provides the largest vertical resolution. For our system, the theoretical vertical resolution $\Delta z = v_s/2B$ corresponds to the minimum separation distance at which two reflectors, differing in magnitude by a factor of at least 20, can be resolved.

Measurements at four different incidence angles at C-band frequencies indicated that snow layering information can be obtained at $\theta < 15°$, whereas measurements at $\theta = 30$ and $45°$ are dominated by the reflection from the snow–ground interface. These measurements gave a qualitative indication that surface scattering dominated for $\theta < 15°$; however, measurements at more incidence angles θ would be required for quantitative interpretation.

Measurements in four different snowpacks indicated that the FMCW radar was capable of measuring reflections from the entire snowpack in a wide range of conditions. The major radar reflections occurred near large changes in hardness, density, grain size and type. Reflections were measured from a depth hoar layer and a melt–freeze crust. This study indicates that FMCW radar measurements can provide useful information about snowpack stratigraphy; however, quantitative interpretation of layer properties remains difficult. These measurements indicate that a C-band FMCW radar system can penetrate a wide range of snowpack types, and previous work (e.g. Gubler and Hiller, 1984; Holmgren *et al*., 1998; Marshall *et al*., 2004b) shows that snow depth and SWE can be estimated with reasonable accuracy. Ku-band measurements work very well in dry snow, and provide detailed layering information. These measurements will be important for interpreting narrowband active radar measurements from airborne platforms, as they show that the signal can be dominated by reflections from various locations within the snowpack, depending on conditions. These measurements will also help researchers to choose optimal measurement parameters tailored to the snowpack information they are interested in.

ACKNOWLEDGEMENTS

Kelly Elder and Don Cline made it possible to reach all of the field sites with our equipment, and Nate Mullherein assisted in the field during IOPs 1 and 2. The comments of two anonymous reviewers improved this manuscript. This work was funded by NASA Earth Systems Science Fellowship R-ESSF/03-0000-0026.

REFERENCES

Cline D. 2000. The NASA Cold Land Processes mission. *Eos Transactions AGU* **81**(48): fall meeting supplement, H52E–02.

Ellerbruch DA, Boyne HS. 1980. Snow stratigraphy and water equivalence measured with an active microwave system. *Journal of Glaciology* **26**(94): 225–233.

Gubler H, Hiller M. 1984. The use of microwave FMCW radar in snow and avalanche research. *Cold Regions Science and Technology* **9**: 109–119.

Holmgren J, Sturm M, Yankielun NE, Koh G. 1998. Extensive measurements of snow depth using FM-CW radar. *Cold Regions Science and Technology* **27**: 17–30.

Koh G, Jordan R. 1995. Sub-surface melting in a seasonal snow cover. *Journal of Glaciology* **41**(139): 474–482.

Koh G, Yankielun NE, Baptista AI. 1996. Snow cover characterization using multiband FMCW radars. *Hydrological Processes* **10**: 1609–1617.

Marshall HP, Koh G, Forster R. 2004a. *CLPX-ground: ground-based frequency modulated continuous wave (FMCW) radar*. NSIDC Digital Media, Boulder, CO, USA.

Marshall HP, Koh G, Forster R. 2004b. Estimating alpine snowpack properties using FMCW radar. *Annals of Glaciology* (in press).

Stove A. 1992. Linear FMCW radar techniques. *IEEE Proceedings, F (Radar and Signal Processing)* **139**(5): 342–350.

Tiuri M, Sihvola A, Nyfors E, Halikaiken M. 1984. The complex dielectric constant of snow at microwave frequencies. *IEEE Journal of Oceanic Engineering* **OE-9**(5): 377–382.

Ulaby F, Moore R, Fung A. 1986. *Microwave Remote Sensing: Active and Passive*, vols I–III. Artech House: Norwood, MA.

